

In-situ Antenna Pointing Angle Calibration for Q-band Satellite Ground Station

Fan, Wei; Yang, Wen ; Meng, Lizhu ; Eggers, Patrick Claus Friedrich; Zhang, Fengchun; Syrytsin, Igor Aleksandrovich; Kristmundsson, Johannus; Geng, Suiyan ; Pedersen, Gert Frølund

Published in:

I E E E Antennas and Wireless Propagation Letters

DOI (link to publication from Publisher):

[10.1109/LAWP.2020.2996950](https://doi.org/10.1109/LAWP.2020.2996950)

Publication date:

2020

Document Version

Accepted author manuscript, peer reviewed version

[Link to publication from Aalborg University](#)

Citation for published version (APA):

Fan, W., Yang, W., Meng, L., Eggers, P. C. F., Zhang, F., Syrytsin, I. A., Kristmundsson, J., Geng, S., & Pedersen, G. F. (2020). In-situ Antenna Pointing Angle Calibration for Q-band Satellite Ground Station. *I E E E Antennas and Wireless Propagation Letters*, 19(7), 1246-1250. Article 9099386. <https://doi.org/10.1109/LAWP.2020.2996950>

General rights

Copyright and moral rights for the publications made accessible in the public portal are retained by the authors and/or other copyright owners and it is a condition of accessing publications that users recognise and abide by the legal requirements associated with these rights.

- Users may download and print one copy of any publication from the public portal for the purpose of private study or research.
- You may not further distribute the material or use it for any profit-making activity or commercial gain
- You may freely distribute the URL identifying the publication in the public portal -

Take down policy

If you believe that this document breaches copyright please contact us at vbn@aub.aau.dk providing details, and we will remove access to the work immediately and investigate your claim.

In-situ Antenna Pointing Angle Calibration for Q-band Satellite Ground Station

Wei Fan, Yang Wen, Lizhu Meng, Patrick Eggers, Fengchun Zhang, Igor A. Syrytsin, Johannus Kristmundsson, Suiyan Geng and Gert F. Pedersen

Abstract—Exploration of millimeter-wave (mmWave) bands has gained a significant interest in satellite communications. mmWave satellite communication link quality is highly sensitive to the pointing angle of the antenna in the ground station, due to its high directivity. For the multi-antenna ground station design, it is also of importance to know pointing angles and angle difference of all antenna elements. However, it is challenging in the real-world setup. In this paper, we propose a novel calibration technique to estimate the electrical antenna pointing angle of the in-situ ground station based on the received signal power pattern on the ground station, which is time-variant according to the satellite in-orbital motion. The proposed algorithm is numerically simulated and experimentally validated, demonstrating its effectiveness for the in-situ antenna pointing angle calibration.

Index Terms—Satellite communication, in-situ antenna pointing angle calibration, beacon receiver design, radio propagation.

I. INTRODUCTION

The ever-growing need for data-rate in satellite communications is promoting the exploitation of millimeter-wave (mmWave) frequencies, thanks to the large available bandwidth [1], [2]. However, mmWave systems are severely affected by different atmospheric impairments, especially under unfavorable weather conditions. Besides the attenuation due to atmosphere, the satellite radio signal might also suffer from scattering by rain drops, hails, snowflakes, etc, since the wavelength at the mmWave band becomes comparable to the dimension of those objects in the atmosphere. Knowing behavior of propagation channel in the earth-space link is crucial for the system design and development, e.g. to determine the link margin, availability and quality of service, etc. Therefore, extensive propagation experiments have been reported to understand the channel characteristics [1]–[5].

Antennas employed in the ground station typically present high gain, high directivity and very narrow beam-width to meet the link budget requirement of the satellite link. Therefore, antenna pointing angle of the ground station should be carefully calibrated and aligned in practical installation to ensure that it is precisely pointing to the target satellite direction, e.g. within an accuracy of 0.1° . Even a small deviation in the pointing angle might lead to misalignment of ground station and the satellite, resulting in link budget issues. However, this accuracy requirement might be too demanding in the

practical setup, even with dedicated installations. Using multi-antenna to increase link quality is an established and popular technique in terrestrial wireless communications, where diversity combination schemes are extensively exploited. For satellite links at mmWave bands, we can also utilize multiple antennas to exploit diversity, even at a smaller distance due to its small wavelength [2]. To further de-correlate received satellite signals, the antennas employed on the ground station, though approximately pointing to the same angle, might be intentionally tilted with a small difference, e.g. within 1° . However, it is practically challenging to ensure the accuracy of tilting angle of the in-situ multi-antenna system. Land surveying with elaborate geodetic type geometry equipment can be employed to determine the mechanical pointing angle accurately with extensive efforts, which might differ from the electrical center pointing angle. Worse still, such highly accurate equipment is typically not available for a low-cost ground station. In [6], a method was proposed to determine pointing angle by using the sun as a signal source, with the help of an external radio frequency power meter. In [7], [8], a two-way satellite communication system was utilized to align the pointing angle and polarization of the ground station antenna. Unmanned Aerial Vehicles (UAVs) were proposed for in-situ antenna measurement and testing in [9], which allows the evaluation of the antenna radiation pattern in realistic conditions. However, high directivity of the ground station antenna, large measurement range, and link budget issues at mmWave frequencies are still concrete challenges for the in-situ UAV-based antenna measurements.

Communication satellites are only quasi geostationary, e.g. the Alphasat satellite [1], [3] exploited in our measurement campaign. The satellite is not stationary seen from the earth, but rather presents a daily movement trajectory that depends on the orbit inclination. The received signal power on the ground stations will be highly sensitive to the satellite in-orbital movement due to narrow beamwidth of the antenna in the ground station, making it possible to detect the pointing angle based on its time-variant received power. In this paper, we propose a novel calibration technique to estimate the antenna pointing angle of the in-situ ground stations.

II. METHOD

The Q-band beacon signal transmitted by the Alphasat is a constant power continuous wave (CW) signal at 39.402 GHz [1], [3]. A low-cost dual-branch Q-band beacon receiver has been developed and installed in Aalborg University (with location Latitude 57.0120° north, Longitude 9.9943° east and

Wei Fan, Fengchun Zhang, Patrick Eggers, Fengchun Zhang, Igor A. Syrytsin, Johannus Kristmundsson, and Gert F. Pedersen are with the Antenna Propagation and Millimeter-wave Systems (APMS) section, Aalborg University, Denmark. Email: wfa@es.aau.dk

Yang Wen, Lizhu Meng, and Suiyan Geng are with School of Electrical and Electronic Engineering, North China Electric Power University, China.

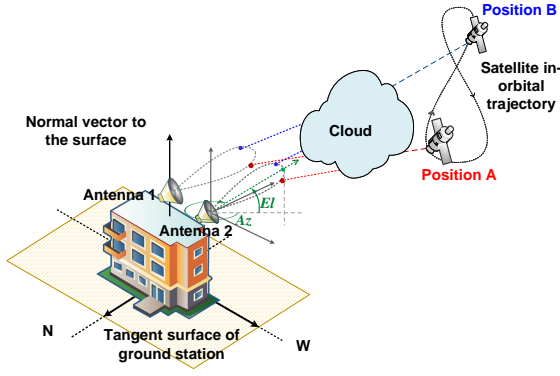


Figure 1. An illustration of the satellite-earth communication link.

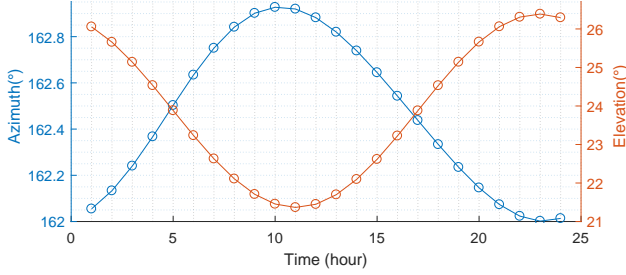


Figure 2. Time-variant azimuth (light blue curve) and elevation angle (brown curve) along the satellite in-orbital trajectory seen from the ground station.

Altitude 35 m) and it is able to acquire the Q band beacon signal transmitted by of the Alphasat. The beacon receivers on the ground station receive and measure the beacon power in order to extract the induced signal attenuation in the satellite-earth link. The geosynchronous orbit of the Alphasat satellite is inclined on the equatorial plane with a maximum of 3° inclination, and the satellite longitude is 25° East. The average azimuth and elevation angle viewed from the installation site is 162.4652° and 23.7704° , respectively.

The geometry of satellite-earth link is illustrated in Fig. 1. The Alphasat in-orbital location is recorded per hour and available in [5]. The latitude-longitude-altitude coordinates of the satellite in-orbital trajectory in a day can be converted to local East, North, Up (ENU) coordinate system using the coordinate transformation. Note that both the satellite and ground station location are converted to the same ENU coordinates for analysis. As shown in Fig. 2, the elevation angle and azimuth angle change are around 5.02° and 0.87° over a day (January 11th 2020), respectively.

Due to the incoming angular change introduced by the satellite motion and narrow beamwidth of the receiving antenna, the received signal power on the ground stations will vary. Therefore, the antenna pointing angle can be estimated according to the time-variant received signal power in principle. Assuming a pure LOS propagation in the satellite-earth link, the time-variant received signal power due to satellite in-orbital motion is shown in Fig. 3. In Fig. 3, the ground station antenna is pointing to the geometrical center of the satellite motion orbit. Further, the tilting angle in azimuth and elevation (i.e. the deviation from the pointing angle) are denoted as Δ_ϕ and Δ_θ , respectively. The ground station antenna radiation pattern

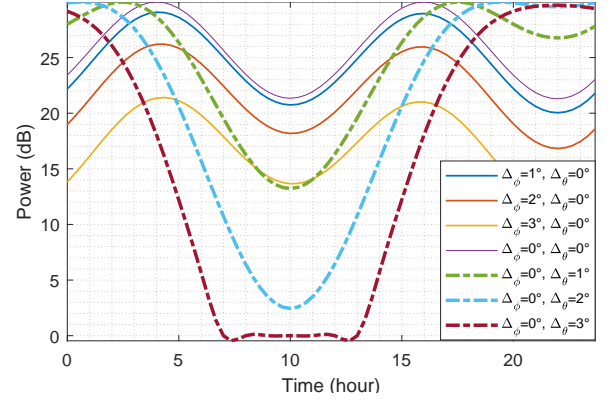


Figure 3. Time-variant received signal power pattern during the satellite in-orbital motion in the ground station.

is calculated following 3GPP recommendation with 3° and 3.5° half power beamwidth (HPBW) in the E and H plane (to mimic the horn antenna employed in the measurement campaign as explained later), respectively [10]. As shown in Fig. 3, the time-variant received signal power is periodic and highly sensitive to the tilting angle, making it possible to determine the in-situ antenna pointing angle in the ground station. Due to azimuth angle deviation, the received signal power is significantly attenuated, while the pattern remains the same. This is due to the fact that we have a negligible change in azimuth angle in the satellite in-orbital motion. However, the power pattern changes significantly with same power level due to the elevation angle deviation. This is due to the large elevation angle change in the satellite in-orbital motion.

However, the raw received signal in the time domain is significantly affected by the noise in the sky and receiver hardware, making it difficult to track the power pattern directly. Therefore, we need to perform Fourier transform of the measured time-domain data to its Doppler domain, in order to track the LOS component and extract the corresponding received power pattern over satellite in-orbital trajectory. The Doppler shift of the LOS path due to the satellite in-orbital motion can be calculated as:

$$f_d = \cos(\theta) \frac{\pm v}{c} f_c \quad (1)$$

where θ is the instantaneous elevation angle of the satellite in the in-orbital trajectory, v the velocity of the satellite (with $+$ indicating satellite moving towards earth and $-$ indicating moving away from earth), c the speed of light and f_c the CW frequency 39.402 GHz. The speed v can be calculated according to the satellite in-orbital trajectory. Note that the Doppler frequency of the LOS component is time-variant due to the time-variant elevation angle and speed due to the satellite motion. Once the Doppler of the LOS path is tracked, the corresponding received signal power can be further extracted and used for antenna pointing angle calibration.

III. MEASUREMENT CAMPAIGN AND RESULTS

A. Beacon Receiver

The dual-branch I/Q satellite beacon receiver is based on the software defined radio (SDR) architecture, making use of

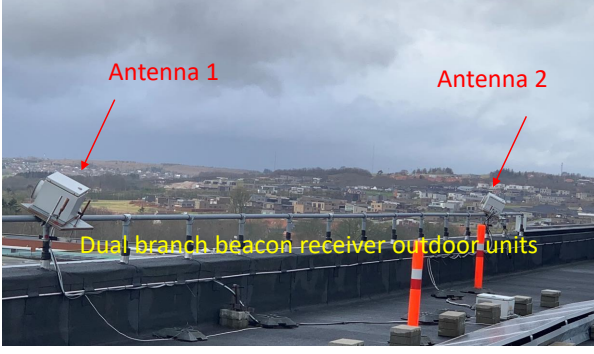


Figure 4. A photo of the dual-branch beacon receiver outdoor units.

off-the-shelf commercial components. The designed receiver offers phase-coherent signal measurement of the two branches with a dynamic range of more than 35 dB and system phase error within 10° . Unlike most single branch satellite beacon receiver reported in the literature, our unique dual-branch design offers possibility to investigate micro diversity (i.e. with a small site distance) in a macro link setting (i.e. for a large distance between satellite and ground station). The Q-band dual branch receiver front-end consists of two horn antennas (model Flann 22880-F), as shown in Fig. 4. The horn antenna has a gain of 34 dBi, 3° and 3.5° HPBW in the E and H plane, respectively. The signals are down-converted and fed to a dual channel direct sampling SDR which further samples them and stores them for post-processing in a computer. The sampling frequency is set to $f_s = 96$ kHz.

In the practical installation, both horn antennas are set to point to the geometry center of the satellite orbit. To track the satellite in-orbital movement, complicated tracking mechanism is required if highly directive antennas are employed. As an alternative, we can use less directive antennas in the ground station to avoid the need for complicated tracking. However, such simple structure would suffer from the link budget issue. Our dual-channel receiver design exploits multi-antenna strategies to help alleviate the problem. The two horn antennas can be separated up to 20 m (i.e. 10 m cable connected to each horn antenna) in the setup to exploit space diversity, as shown in Fig. 4. Both antennas are pointing to the satellite orbital trajectory center, with a very small angle difference, to exploit angle diversity. For the LOS satellite link condition, the dual antenna can only offer 3 dB array gain. We can achieve wider coverage of the satellite link and therefore lower power fluctuation over a day by angle diversity. In the obstructed-LOS condition, we can achieve less fading with the dual antenna system (i.e. space and angle diversity). However, the exact pointing angles and the tilt angle difference of the two horn antennas are difficult to estimate after installation in practice, which motivates our work to develop an accurate in-situ antenna pointing angle calibration method. A back-to-back calibration measurement was performed for the dual branch receiver before the actual measurement to compensate out the gain difference, which is required to ensure accurate differential signal power measurement in the two branches.

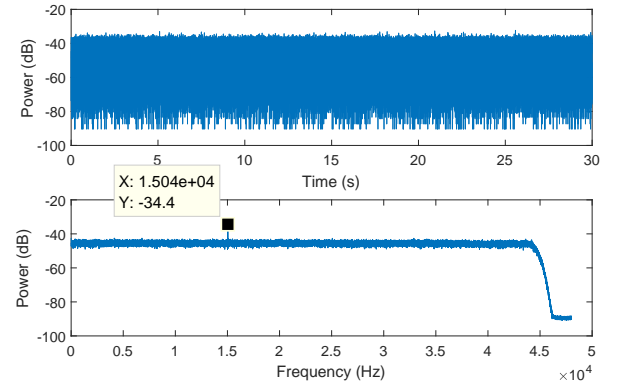


Figure 5. Raw time-domain data recorded over 30s period and its Doppler spectrum received at the first antenna.

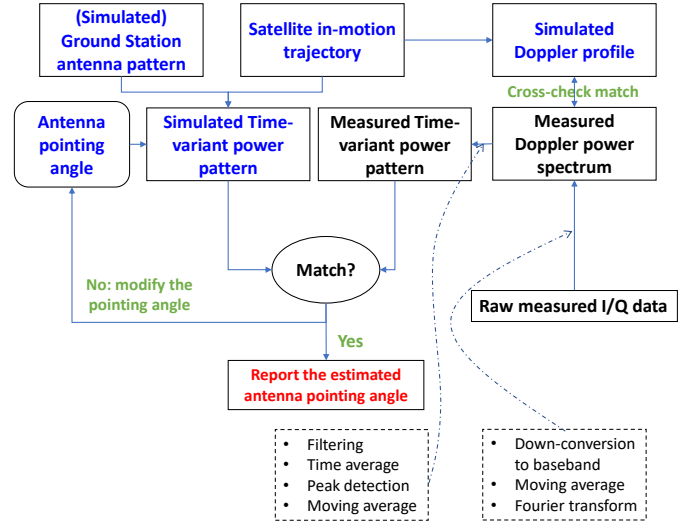


Figure 6. An illustration of the data analysis procedure.

B. Data Analysis

One-day data recorded on the May 26th 2019 was utilized for our validation purpose. The raw measured data received at the first antenna in the time-domain over 30s and its single-sided Doppler spectrum are shown in Fig. 5 as an example. As we can see, the received signal is very noisy in the time domain, making it not possible to track the LOS signal directly, as expected. The noisy data is due to sampling with a wide bandwidth, which is intentionally employed to allow flexibility in post-processing for choosing the effective noise bandwidth to enable flexibility of tracking signal changes. In the Doppler profile, the LOS component with Doppler frequency around 15 KHz can be clearly observed. Note that the signal is deliberately moved to audio carrier frequency to avoid the possible DC leakage problem in the down conversion process.

The data processing procedure is shown in Fig. 6. The length of time segment for performing Fourier analysis should also be carefully chosen. In principle, a longer time segment would offer higher resolution in the Doppler domain. However, a longer time segment also means a large Doppler shift over time, due to the Doppler shift over time. In the paper, a time segment of 3s is adopted. The raw measured data is

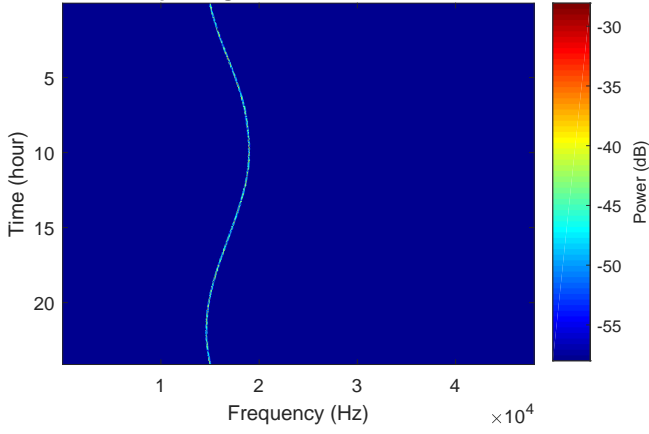


Figure 7. Spectrogram of the received signal at the antenna 1.

digitally down-converting to around the baseband from the IF band, by introducing a frequency shift of 14.654 KHz. The frequency shift value is set to the lowest Doppler frequency of the LOS signal over a day, as determined later. After the down-conversion, the highest Doppler frequency of the LOS signal over a day is around 4.2 KHz. To reduce the wideband integrated noise and improve overall SNR, a decimation is implemented by applying a moving average window in the time-domain. The window length is set to 9 to ensure that Nyquist sampling criteria is still respected ($f_s = 96 \text{ KHz}/9 = 10.7 \text{ KHz}$). After applying the Fourier transform, we can obtain the Doppler profile. Furthermore, to reduce the effect of noise, an average of 10 Doppler power spectra (each corresponding to 3s time segment) was performed. The spectrum of received signal at the first antenna is shown in Fig. 7.

To extract the power corresponding to the LOS signal, a band-pass filter centered at the tracked LOS Doppler with 12 Hz bandwidth was applied. The LOS Doppler in the measured data was tracked (via peak searching), extracted and compared with the simulated LOS Doppler profile in Fig. 8. The simulated profile is shifted in time due to several reasons. The Earth rotation period around its axis is not precisely 24 hours, but rather around 23 hours and 56 minutes [4]. This will effectively introduce a shift of around 8.5 hours over 230 days. Furthermore, satellite position is predicated, which might be inaccurate [4], and its inaccuracy will propagate over time. The deviation in Doppler shift between the measured and simulated (with correction) Doppler profile is up to 117.3 Hz in a day, which indicates a good agreement. To extract the LOS power in the noisy data, a moving average window of 45s was further applied. The received power patterns corresponding to the LOS component for the two received antennas are shown in Fig. 9. To estimate the antenna pointing angle, we can sweep the pointing angle in the simulation, and perform a brute-force search for the best match between the simulated and measured power patterns, as illustrated in Fig. 6. The best match is found when we have the highest correlation. The tilted pointing angles are found to be $\Delta_{\theta_1} = -0.3^\circ$ and $\Delta_{\phi_1} = -1.3^\circ$ for the first antenna, and $\Delta_{\theta_2} = -0.1^\circ$ and $\Delta_{\phi_2} = -1.6^\circ$ for the second antenna, respectively. Therefore, a pointing angle difference of 0.1° in the elevation and 0.3° in the azimuth angle can be found, respectively. A good agreement between

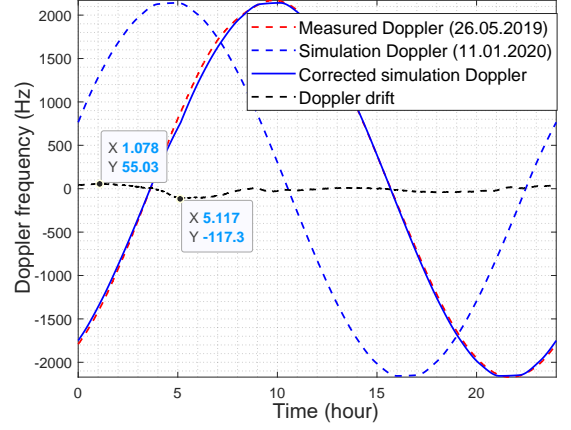


Figure 8. Measured and simulated LOS Doppler frequency shift due to the satellite in-orbital motion.

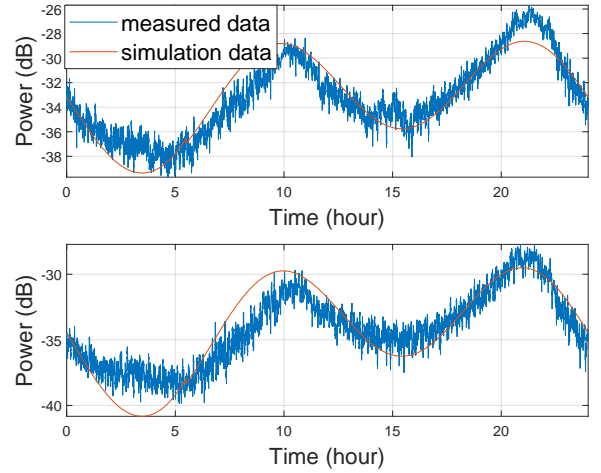


Figure 9. Measured and simulated received signal power patterns for antenna 1 (top) and antenna 2 (bottom).

the measured and fitted simulated patterns can be observed for both antennas. The deviation between the measured and simulated power pattern are mainly introduced by the noise in the sky, inaccuracies in the simulated antenna pattern, and receiver hardware impairment.

IV. CONCLUSION

In-situ antenna pointing angle calibration is challenging, where dedicate land surveying techniques are usually expensive and not able to determine the true electrical pointing angle. In this paper, a novel strategy is proposed based on the principle that the received power pattern is highly sensitive to the satellite in-orbital movement. The idea is numerically simulated, and experimentally demonstrated with measured data after applying noise reduction strategies in the measured data. A good agreement between the simulated and measured time-variant power patterns is achieved. Furthermore, a tilt angle difference between the two receive antennas as small as 0.09° in the elevation and 0.31° in the azimuth were found, indicating that the proposed method is highly accurate and robust for practical application.

REFERENCES

- [1] T. Rossi, M. De Sanctis, M. Ruggieri, C. Riva, L. Luini, G. Codispoti, E. Russo, and G. Parca, "Satellite communication and propagation experiments through the alphasat q/v band aldo paraboni technology demonstration payload," *IEEE Aerospace and Electronic Systems Magazine*, vol. 31, no. 3, pp. 18–27, March 2016.
- [2] A. D. Panagopoulos, P. M. Arapoglou, and P. G. Cottis, "Satellite communications at ku, ka, and v bands: Propagation impairments and mitigation techniques," *IEEE Communications Surveys Tutorials*, vol. 6, no. 3, pp. 2–14, Third 2004.
- [3] C. G. Riva and L. Luini, "Thermal effects on a 4.2 m center-fed cassegrain antenna strut in the alphasat ka- and q/v-band aldo paraboni propagation measurements," *IEEE Transactions on Antennas and Propagation*, vol. 66, no. 7, pp. 3700–3705, July 2018.
- [4] V. Pek, V. Brazda, and O. Fiser, "Description of alphasat satellite space motion and its consequences for signal reception," in *2016 26th International Conference Radioelektronika (RADIOELEKTRONIKA)*, April 2016, pp. 464–469.
- [5] "Satellite motion charts for ALPHASAT based on TLE data."
- [6] H. Yokotsuka, K. Fukue, M. Sone, K. Cho, R. Matsuoka, N. Sudo, H. Shimoda, and Y. Matsumae, "A proposal on antenna alignment calibration method of a receiving ground station for earth observation satellite," *IEEE Transactions on Electronics, Information and Systems*, vol. 126, pp. 14–23, 2006.
- [7] L. Gerlinger, E. Greilinger, and C. Hausleitner, "Method and system for the alignment of an earth station antenna with a satellite antenna," Mar. 9 2010, uS Patent 7,675,462.
- [8] A. Frost, S. Wheelis, J. Mueller, and G. Myers, "Remote satellite terminal with antenna polarization alignment enforcement and associated methods," Jul. 1 2014, uS Patent 8,768,242.
- [9] M. G. Fernandez, Y. A. Lopez, and F. L. Andres, "On the use of unmanned aerial vehicles for antenna and coverage diagnostics in mobile networks," *IEEE Communications Magazine*, vol. 56, no. 7, pp. 72–78, July 2018.
- [10] G. R. A. N. W. Group *et al.*, "Study on channel model for frequencies from 0.5 to 100 ghz (release 15)," 3GPP TR 38.901, Tech. Rep., 2018.